

# Enhanced Ubiquitinylation of Heat Shock Protein 90 as a Potential Mechanism for Mitotic Cell Death in Cancer Cells Induced with Hypericin

Michael Blank,<sup>1</sup> Mathilda Mandel,<sup>2</sup> Yona Keisari,<sup>1</sup> Daniel Meruelo,<sup>3</sup> and Gad Lavie<sup>2,3</sup>

<sup>1</sup>Department of Human Microbiology, Sackler Faculty of Medicine, Tel-Aviv University, Tel Aviv, Israel; <sup>2</sup>Institute of Hematology and Blood Transfusion Center, Sheba Medical Center, Tel-Hashomer, Israel; and <sup>3</sup>Department of Pathology, New York University Medical Center, New York, New York

## ABSTRACT

A unique property of the photodynamic signal transduction inhibitor hypericin is functionality in the dark. We show in tumor cells that hypericin targets the heat shock protein (Hsp) 90 chaperone but not Hsp70 (Hsc70) to enhanced ubiquitinylation. As a consequence Hsp90 chaperone functionality is abrogated and the client proteins, mutant p53, Cdk4, Raf-1, and Plk, are displaced from complexes with Hsp90, destabilized, and degraded via a proteasome-independent pathway. Decline in Raf-1 prevents downstream activation of extracellular signal-regulated kinase 1/2 kinases, the Ras/Raf pathway is inhibited, and tumor cell proliferation is arrested. The cells exhibit multiple aberrations including retardation at G<sub>2</sub>-M, increased cell volume, and multinucleation, all of which are hallmarks of mitotic cell death. The studies demonstrate that ubiquitinylation of Hsp90 inactivates the chaperone, destabilizes the plethora of client proteins, and creates deficiencies in multiple unrelated cellular functions. This combination constitutes a mechanism by which hypericin generates mitotic cell death in cancer cells.

## INTRODUCTION

Treatment of cancerous cells with chemotherapeutic agents such as cisplatin (1), daunorubicin (2), and paclitaxel (3), as well as radiotherapy with high dose  $\gamma$  radiation, can kill tumor cells via a newly described mitotic catastrophe or MCD<sup>4</sup> mechanism (4, 5). This phenomenon, which prevails in many tumors bearing mutant p53 and which exhibit resistance to genotoxic agents, is characterized by cell accumulation at G<sub>2</sub>-M, increased cell volume, and multinucleation (6). A variety of seemingly unrelated cellular functions appear to be altered as cells approach mitotic death. The G<sub>1</sub>-S checkpoint diminishes in activity, cells are delayed at G<sub>2</sub>, apoptosis is uncoupled, and polygenomic giant cells are formed (7). The processes, which lead to development of these abnormal polykaryons remain controversial, and theories fluctuate between aberrant endomitotic replication cycles and cell fusion (5).

The anticancer activities of the signal transduction inhibitor hypericin, a photodynamic diantraquinone, elicit light-dependent inhibition of protein kinase C (8) and Erk1/2 MAP kinases (9). However, hypericin is unique in its ability to also maintain activity within biological systems in the absence of light (Refs. 10, 11; dark effects). It results in a portfolio of antitumoral (10), antimetastatic,<sup>5</sup> immunomodulatory (12), and antiviral (13, 14) activities *in vitro*, and in animal models in the dark.

In exploring mechanisms for its anticancer activities we considered that hypericin can cause reduction in intracellular pH by proton

transfer to surrounding molecules (15) leading to pH-dependent structural changes in proteins (16). Furthermore, in cells this compound localizes to the endoplasmic reticulum and Golgi apparatus (17), which are folding sites of newly synthesized proteins. The broad range of activities may, thus, result from hypericin targeting chaperone networks. One abundant chaperone that assists in protein folding and protects *de novo* synthesized proteins from catabolism is Hsp90 (18, 19). This chaperone is pivotal for stability and function of a large group of client proteins including ser/thr kinases, tyrosine kinases, mutated p53, cyclin D-associated Cdk4 (20) and Cdk6, and wild-type Plk (21). Replication mechanisms in cells that lose Hsp90-protective function are severely compromised, disabling cell progression through the cell cycle (22). Indeed, Hsp90 modulators such as geldanamycin or radicicol, which interact with the ATP binding pocket of Hsp90, exhibit potent anticancer effects (18).

In this study we examined the correlation between stability of members of chaperone families and cell functionality in two murine tumor cell models treated with hypericin in the dark. A link through Hsp90 is unraveled between several key cell cycle regulators, which are destabilized as a result of loss of protective chaperone activity leading to MCD. The potential role of such mechanisms in generating diverse biological activities is discussed.

## MATERIALS AND METHODS

**Reagents.** Monoclonal antibodies to Cdk1, Cdk2, Cdk7, Raf-1, p27<sup>kip1</sup>, Plk, ubiquitin, and polyclonal anticyclin B<sub>1</sub> and anti-Plk (H-152) antibodies (for immunoprecipitations) were obtained from Santa Cruz Biotechnology, Inc. (Santa Cruz, CA); monoclonal antibodies to p53, cdk4, cyclin A, and proliferating cell nuclear antigen were from Oncogene (Boston, MA). Anti-HSP-90 and anti-Hsc70 antibodies were purchased from StressGen Biotechnologies (Victoria, British Columbia, Canada); anti-Erk1/2 MAP kinases (antibody Erk1/2-CT) and anti-Active MAP kinase pAb (pTEpY) polyclonal antibodies from Upstate Biotechnology (Lake Placid, NY) and from Promega (Madison, WI), respectively. Anti-p50<sup>cdc37</sup> antibody was a gift from Dr. Nicholas Grammatikakis (Queen's University, Kingston, Ontario, Canada). Secondary horseradish peroxidase-conjugated or FITC-labeled antibodies were from Jackson ImmunoResearch Laboratories, Inc. (West Grove, PA).

Hypericin (10, 11-dimethyl-1, 3, 4, 6, 8, 13-hexahydroxy-naphtho-dianthrone) was synthesized by Yehuda Mazur (Department of Organic Chemistry, Weizmann Institute of Science, Rehovot, Israel) as described previously (12). The compound was dissolved in 70% aqueous ethanol to a 3 mg/ml stock solution. Subsequent dilutions were made in sterile double distilled H<sub>2</sub>O to obtain a final ethanol concentration <0.5%.

[<sup>35</sup>S]methionine/cysteine NEG-772 EASYTAG express protein labeling mix was purchased from Perkin-Elmer Life Sciences (Boston, MA) and the proteasome inhibitor MG132 from Calbiochem (Darmstadt, Germany).

**Cell Lines and Culture Conditions.** Murine DA3 mammary adenocarcinoma cell line was obtained from Dr. Diana Lopez (University of Miami School of Medicine, Miami, FL), SQ2 squamous cell carcinoma cell line was generated in our laboratory (10), and B16.F10, a highly metastatic melanoma cell line, from Dr. Lea Eisenbach (Weizmann Institute). All of the cell lines were grown in DMEM supplemented with 10% fetal bovine serum, 2 mM L-glutamine, and 100 units/ml penicillin-streptomycin (Life Technologies, Inc., Paisley, Scotland). After administration of hypericin the cultures were maintained in strict darkness (ambient light kept  $\leq 0.03$  mW/cm<sup>2</sup>) throughout the entire duration of the experiments. Light incidence was measured with an IL 1350 Radiometer/Photometer (International Lighting, Newburyport, MA).

Received 4/3/03; revised 9/14/03; accepted 9/19/03.

The costs of publication of this article were defrayed in part by the payment of page charges. This article must therefore be hereby marked *advertisement* in accordance with 18 U.S.C. Section 1734 solely to indicate this fact.

**Requests for reprints:** Gad Lavie, Institute of Hematology and Blood Transfusion Center, Sheba Medical Center, Tel-Hashomer 52621, Israel. Phone: 972-3-5302178; Fax: 972-3-5303072; E-mail: gad.lavie@sheba.health.gov.il.

<sup>4</sup>The abbreviations used are: MCD, mitotic cell death; BrdUrd, bromodeoxyuridine; Cdk, cyclin-dependent kinase; Erk, extracellular signal-regulated kinase; Hsp, Heat shock protein; Hsc70, heat shock cognate protein; Plk, Polo-like kinase; MAP, mitogen-activated protein; RT-PCR, reverse transcription-PCR.

<sup>5</sup>M. Blank, G. Lavie, M. Mandel, S. Hazan, A. Orenstein, D. Mervelo, and Y. Keisari. Antimetastatic activity of the photodynamic agent hypericin in the dark, manuscript in preparation.

**Cell Proliferation and Viability Assays.** DNA synthesis measured as BrdUrd incorporation was assayed on cells grown on glass coverslips and pulsed with BrdUrd. Incorporation of BrdUrd into DNA was visualized by immunostaining with monoclonal antibromo-deoxyuridine antibody followed by FITC-conjugated rabbit antimouse F(ab')<sub>2</sub> using a commercial kit (Amersham, Piscataway, NJ).

Cell viability was assessed using the Hemacolor assay (reagents obtained from Merck, Darmstadt, Germany) as described previously (16). The percentage of cells remaining in hypericin treated cultures (or in untreated samples) is presented as percentage of cell viability using the formula:

$$\% \text{ Cell Viability} = [1 - O.D.(\text{hypericin})/O.D.(\text{Untreated})] \times 100\%$$

**Cell Cycle Analyses.** Cellular DNA content was determined by cell staining with propidium iodide using a Coulter DNA-Prep kit (Beckman Coulter Int. S.A., Nyon, Switzerland). Cell cycle distribution was determined using Coulter EPICS XL-MCL flow cytometer (Coulter) and Multicycle software (Phoenix, San Diego, CA) for data analysis. Polykaryons occurring during MCD were visualized by concomitant staining of cell cultures with Hemacolor reagents (10).

**Immunoprecipitation and Western Blot Analysis.** Nuclear and cytosolic extracts were prepared from DA3 and SQ2 cells grown to confluence; cytosolic extracts using buffer A [10 mM HEPES (pH 7.9), 10 mM KCl, 1 mM EDTA, 1 mM EGTA, 1 mM DTT] and complete Protease Inhibitor mixture, 40 µg/ml (Boehringer, Mannheim, Germany), containing 0.6% NP40. Nuclear extracts were prepared by dissolution of nuclei in buffer C [20 mM HEPES (pH 7.9), 400 mM KCl, 1 mM EDTA, 1 mM EGTA, 1 mM DTT, and complete Protease Inhibitor mixture 40 µg/ml]. The protein content was calibrated using the BCA protein assay reagent kit (Pierce, Rockford, IL). Samples were separated on 10–15% SDS-PAGE and transblotted onto nitrocellulose filters (Schleicher & Schuell, Dassel, Germany). Equal protein loading was verified by staining with Ponceau S (Sigma, St. Louis, MO). The membranes were probed with several primary antibodies, with peroxidase-tagged second antibodies and developed with enhanced chemiluminescence (SuperSignal West Pico Chemiluminescent Substrate; Pierce).

Immunoprecipitates were prepared from cytosolic extracts. After overnight incubation with primary antibodies, samples were immobilized with Protein A/G PLUS-Agarose (Santa Cruz Biotechnology) at 4°C. Immunoprecipitated proteins were separated on 10% SDS-PAGE and subjected to Western blot analyses.

**Metabolic Labeling of Plk.** DA3 cells were cultured in DMEM (met<sup>-</sup>, cys<sup>-</sup>; Life Technologies, Inc.) containing 10% dialyzed FCS and 100 µCi ml<sup>-1</sup> [<sup>35</sup>S]methionine/cysteine for 1 h. The cells were washed with PBS, cultured in chase medium, lysed, and cytosolic extracts prepared. Plk was immunoprecipitated and the precipitates separated on SDS-PAGE. Radiolabeled proteins were visualized by fluorography.

**RT-PCR.** mRNA expression was analyzed using the Titan one-step RT-PCR system (Roche Molecular Biochemicals, Mannheim, Germany). β-Actin served as a reference housekeeping gene. Specific primers were designed from sequences derived from GenBank database using the Primer3 Software (Whitehead Institute) to yield an annealing temperature of 55°C. The specificity of these primers was confirmed using Standard nucleotide-nucleotide BLAST. Primers used were: Plk: 5'-aagtcttgcgtcgaacc-3' (forward) 5'-aggtccctgtgaatgacctg-3' (reverse); Hsp90β: 5'-agaaggctgaggcagacaaa-3' (forward) 5'-ctccaagtcatcatgagcca-3' (reverse); and β-Actin: 5'-atggatgacgatactgct-3' (forward) 5'-atgaggtagtctgacagt-3' (reverse).

Amplified cDNAs were subjected to electrophoresis and photographed under UV light.

**Statistical Analyses.** The data were analyzed using the two-tail Student's *t* test. *P*s < 0.05 were considered statistically significant.

## RESULTS

**Inhibition of Tumor Cell Growth and Induction of MCD by Hypericin in the Dark.** Treatment of DA3 breast and SQ2 squamous carcinoma cells with hypericin for 72 h in strict darkness (to exclude light-induced phototoxicity) had two outcomes. Doses ≤10 µM induced cytostasis; BrdUrd incorporation into DNA declined to below detection (Fig. 1A); and [<sup>3</sup>H]thymidine incorporation into DNA diminished (data not shown). Concentrations >10 µM reduced cell

viability with LD<sub>50</sub> of ~10 µM in SQ2 cells, and 12.5 µM in DA3 cells (Fig. 1B). Complete loss of cell viability in both cell lines occurred after cell exposure to ≥40 µM hypericin.

The proportion of cells sequestered in G<sub>2</sub>-M increased from 28.1% in untreated controls to 41.8% (*P* = 0.025; *n* = 7) after 72 h treatment of DA3 cells with 20 µM hypericin (Fig. 1C). No evidence for occurrence of apoptosis could be detected: sub-G<sub>1</sub> DNA peaks in propidium iodide-stained cells were absent and DNA ladder not noted in agarose gel electrophoresis in both cell lines.

Microscopic analyses revealed the formation of enlarged polynucleated cells in DA3 cells, SQ2 cells, and in B16.F10 melanoma cells (Fig. 1D). Polykaryon abundance began to increase 48 h after administration of ≥10 µM hypericin and peaked at 72 h. The decline in G<sub>1</sub> checkpoint activity, retardation at G<sub>2</sub>-M phase, and multinucleation are hallmarks of MCD (5) and point to induction of this phenomenon by hypericin in the dark.

### Destabilization of Cell Replication Mediators by Hypericin.

Expression of several cell cycling regulators that govern cell progression through the replication cycle were examined in DA3 and SQ2 cells after treatment with hypericin for 72 h. Western blot analyses revealed diminished expression of mutant p53, cdk4, and Raf-1 in DA3 cells (Fig. 2A). Most of these proteins declined to below detection primarily in the cytosolic fraction of the cells in hypericin dose-dependent manners. Catabolism of mutant p53 showed evidence of ubiquitinylation (Fig. 2A, top panel). The mutated nature of p53 in DA3 cells was confirmed by immunofluorescence using the monoclonal PAb 240 anti-p53 antibody (data not shown). Under nondenaturing conditions this antibody has been shown to react selectively with mutant p53 (23, 24).

The cytoplasmic content of Plk, a prominent regulator of mitotic events such as spindle formation, chromosome segregation, and cytokinesis (21), also diminished after the treatment in a hypericin dose-dependent manner (Fig. 2A). Mutant p53, cdk4, Raf-1, and Plk are all client proteins of Hsp90, assisted in folding and subsequently stabilized by this chaperone (20).

Similar effects were noted in the SQ2 cell model in which cellular contents of the Hsp90 client proteins Raf-1 and Plk also declined dramatically after treatment with hypericin in the dark (Fig. 2B). SQ2 cells bear wild-type p53 (not immunostained with PAb 240 anti-p53 antibody). Wild-type p53 has been documented not to form stable complexes with Hsp90 (25) and, indeed, p53 expression in SQ2 cells treated with hypericin was unaltered (data not shown).

The diminution in cytosolic Raf-1 prevents the activating phosphorylation of the downstream p44/42 Erk1/2 MAP kinases. In DA3 cells Erk1/2 phosphorylation dissipated after 72 h of treatment with hypericin, whereas the overall content of Erk1/2 remained unaffected (Fig. 2C). In SQ2 cells the effect was mainly on Erk1 phosphorylation (Fig. 2C). Erk1/2 deactivation deprives cells of several active transcription factors downstream to the mitogen-activated Ras/Raf pathway (26), which are essential for cell proliferation.

The temporal relationship between administration of hypericin to DA3 cells and the enhancement of Hsp90 client protein turnover has been examined for Plk using [<sup>35</sup>S]methionine/cysteine pulse-chase analysis. Cells treated with 10 µM of hypericin were subjected to 1 h of met/cys pulses 12, 24, 48, and 72 h before cell lysis. Plk was immunoprecipitated from the lysates and separated on SDS-PAGE. An autoradiogram of Plk cell content at these different time points is shown in Fig. 2D. The results indicate that whereas Plk synthesized between 12 and 48 h, posthypericin administration increased in content and peaked at 48 h compared with untreated controls; Plk pulsed 72 h before cell lysis was almost completely degraded at an accelerated pace (Fig. 2D, right panel). These data suggest that the treatment with hypericin shortened the half-life of Plk, however, only within the

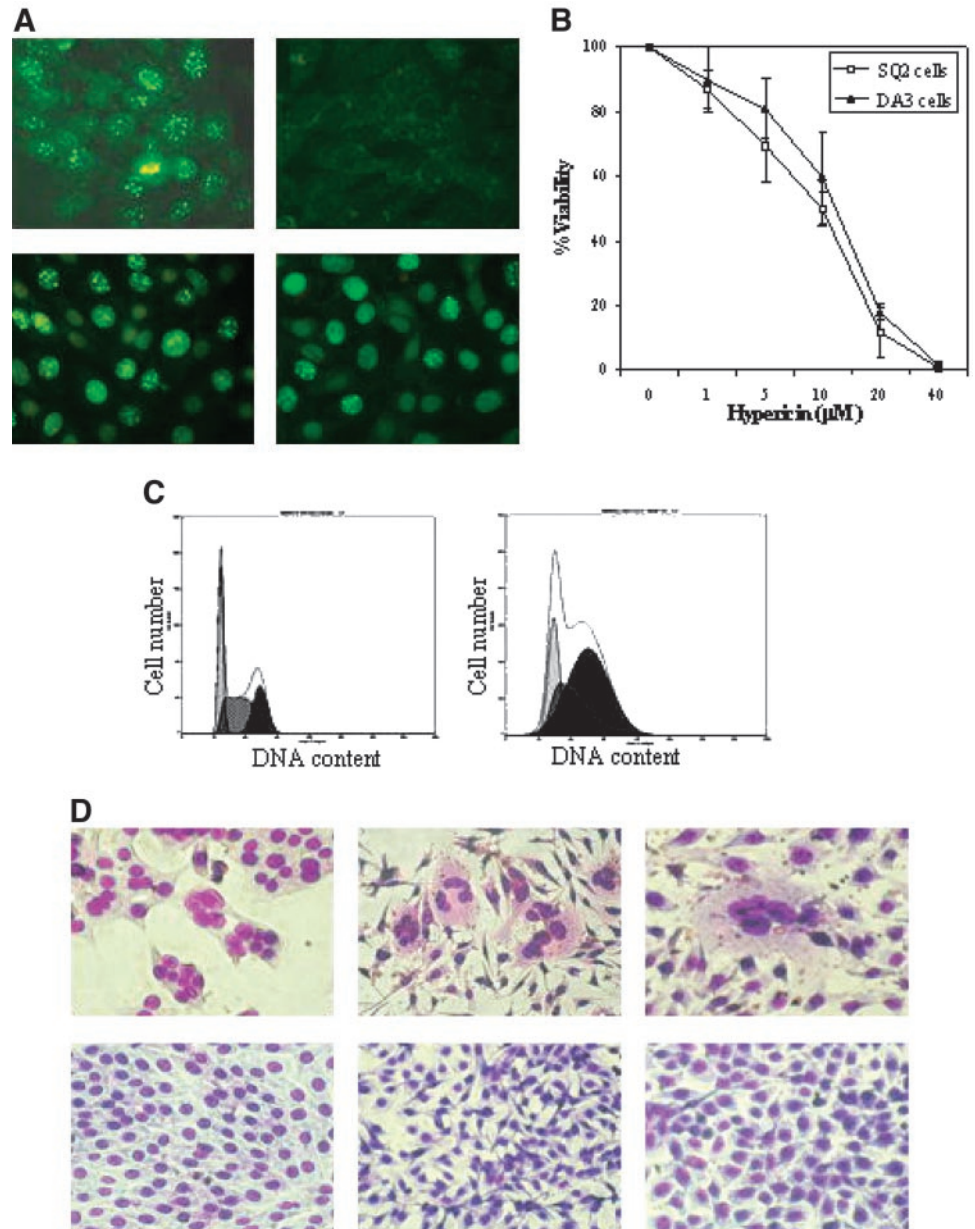


Fig. 1. Induction of tumor cell cytostasis and mitotic death by hypericin. *A*, incorporation of BrdUrd into DNA. DA3 cells stained with anti-BrdUrd after treatment with 10  $\mu\text{M}$  hypericin for 72 h are shown on the *top right panel*, and untreated cells on the *left top panel*. Antiproliferating cell nuclear antigen immunostaining of hypericin-treated cells (*right bottom panel*) and untreated samples (*left bottom panel*) was used as control for nuclear staining. *B*, effects of cell treatment with hypericin for 72 h in the dark on tumor cell viability. *C*, cell cycle analysis of untreated DA3 cells (*left panel*) and after exposure to 20  $\mu\text{M}$  hypericin (*right panel*). *D*, polykaryons, which develop after treatment with hypericin for 72 h in the dark. *Top panel*, hypericin-treated cells; *bottom panel*, untreated controls. *Left panels*, DA3 cells; *middle panels*, B16.F10 cells; *right panels*, SQ2 cells.

last 24 h. The transcription of Plk remained unchanged throughout the 72-h cell treatment with hypericin, (Fig. 2E).

To determine whether the enhanced turnover of Hsp90 client proteins in hypericin-treated cells involves the proteasome pathway, we examined the effects of combinations of hypericin and the MG132 proteasome inhibitor on the cellular content of the Hsp90 client proteins Plk and Raf-1 in detergent soluble and insoluble fractions. Fig. 3A shows that addition of 100 nM of MG132 administered for the last 48 of 72 h cell treatment with hypericin (the highest nonlethal dose of MG132 in a 48 h treatment schedule) enhanced hypericin-induced turnover of each of the two Hsp90 client proteins in the NP40 soluble fraction. Whereas MG132 alone induced accumulation of these client proteins in the NP40 insoluble fraction, no such accumulation was noted in combination with hypericin (Fig. 3B). The presence of MG132 was not found to affect the MCD phenomenon induced by hypericin (data not shown).

The destabilization and enhanced turnover of Hsp90 client proteins was associated with marked declines in the cellular content of additional cell cycling regulators. Cyclin A, cyclin B1, and cyclin H (the

regulatory subunit of cyclin activating kinase; Refs. 27, 28) diminished in a hypericin dose-related manner (Fig. 4), whereas Cdk1, Cdk2, and Cdk7 remained unaltered. The cell content of p27<sup>kip1</sup> also decreased and was associated with elevated cyclin E, predominantly in the nuclei (Fig. 4). This latter combination may have contributed to diminishing residual G<sub>1</sub> checkpoint activity and facilitated cell progression to S phase after treatment with hypericin. mRNA levels of cyclin B<sub>1</sub>, cyclin H, Cdk4, and p27<sup>kip1</sup> were unchanged by the action of hypericin, indicating that reductions in the cellular content of these proteins were not an outcome of diminished transcription (data not shown).

**Hypericin Inactivates Hsp90 via Ubiquitinylation of the Chaperone.** To identify the causes for hypericin-induced diminution in cellular content of the Hsp90 client proteins, we examined possible effects of this compound on intracellular Hsp90. The protein was immunoprecipitated from cytosolic fractions of hypericin-treated DA3 and SQ2 cells with anti-Hsp90 antibody and Western blots developed using an antiubiquitin monoclonal antibody.

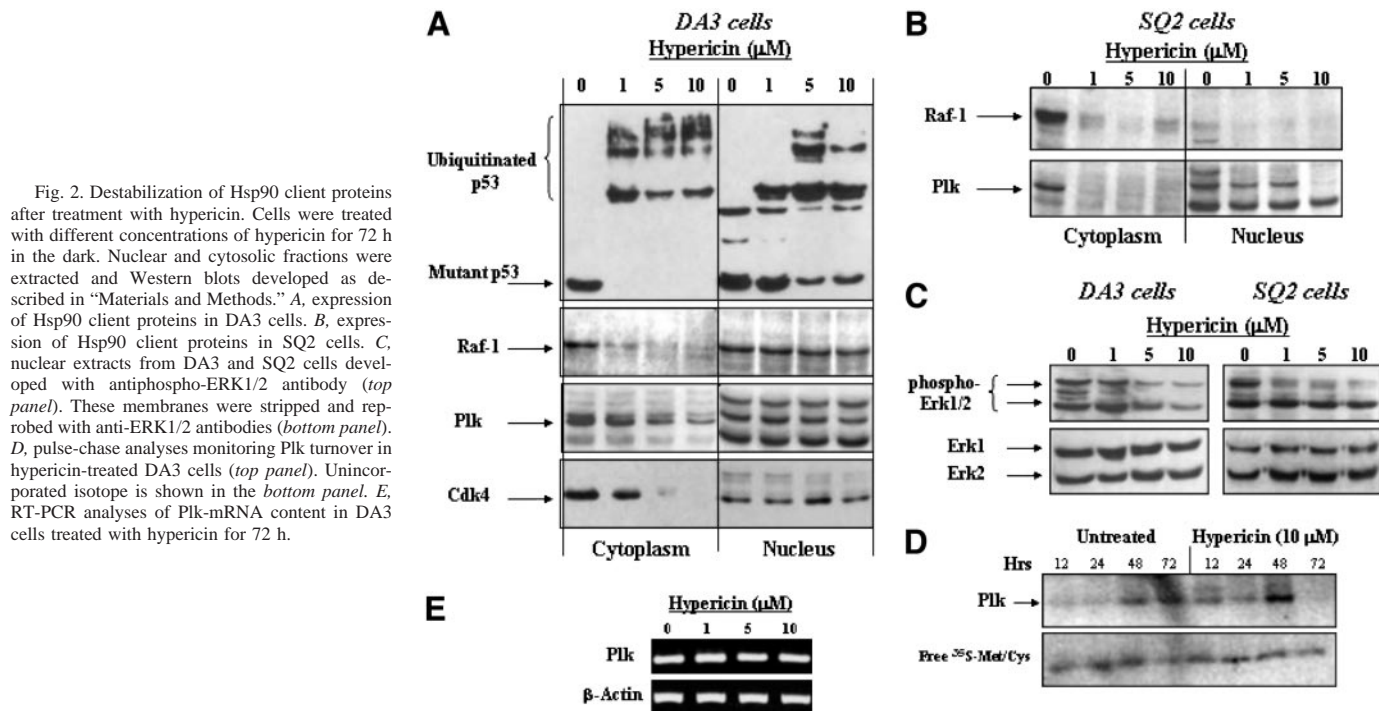


Fig. 2. Destabilization of Hsp90 client proteins after treatment with hypericin. Cells were treated with different concentrations of hypericin for 72 h in the dark. Nuclear and cytosolic fractions were extracted and Western blots developed as described in "Materials and Methods." *A*, expression of Hsp90 client proteins in DA3 cells. *B*, expression of Hsp90 client proteins in SQ2 cells. *C*, nuclear extracts from DA3 and SQ2 cells developed with antiphospho-ERK1/2 antibody (*top panel*). These membranes were stripped and reprobed with anti-ERK1/2 antibodies (*bottom panel*). *D*, pulse-chase analyses monitoring Plk turnover in hypericin-treated DA3 cells (*top panel*). Unincorporated isotope is shown in the *bottom panel*. *E*, RT-PCR analyses of Plk-mRNA content in DA3 cells treated with hypericin for 72 h.

In DA3 cells, Hsp90 was seen to undergo extensive ubiquitinylation (predominantly monoubiquitinylation), which became evident after 48 h of treatment with 10  $\mu\text{M}$  (Fig. 5A, left top panel) and after 72 h of treatment with  $\geq 5$   $\mu\text{M}$  hypericin (Fig. 5A, right top panel). Decreases in Hsp90 became noticeable only after 72 h of cultivation with  $\geq 5$   $\mu\text{M}$  of this compound (Fig. 5A, 2nd right panel). Stripping the nitrocellulose membranes and reprobing with anti-p53 antibody revealed diminished mutant p53 protein in complex with Hsp90 (Fig.

5A, bottom panel) concomitantly with the ubiquitinylation of Hsp90 (Fig. 5A, top panel) and before its own turnover (Fig. 5A, 2nd right panel). Transcription levels of Hsp90 in the cells remained unchanged throughout 72-h treatment periods with hypericin as shown by RT-PCR (Fig. 5C).

Enhancement of Hsp90 ubiquitinylation induced by hypericin was also noted in SQ2 cells. Exposure to hypericin for 72 h resulted in hypericin dose-dependent increases in the amounts of monoubiquitinylation of Hsp90 (Fig. 5B, top panel).

We next examined whether ubiquitinylation of Hsp90 affects its chaperonal functioning, analyzed as capability of Hsp90 to associate with the p50<sup>cdc37</sup> cochaperone. Cytosolic fractions of DA3 and SQ2 cells treated with 10  $\mu\text{M}$  hypericin for 48–72 h, confirmed to contain ubiquitinylation of Hsp90, were immunoprecipitated with anti-p50<sup>cdc37</sup> antibody. The ability of this cochaperone to pull down Hsp90 was examined by immunoblotting with anti Hsp90. Fig. 5D (top panels) shows that the treatment with hypericin strongly diminished the interaction of p50<sup>cdc37</sup> with Hsp90 in both cell lines. The overall contents of p50<sup>cdc37</sup> and also Hsp90 were unaltered in these two cell lines (Fig. 5D, middle and bottom panels).

The ubiquitinylation of Hsp90 by hypericin prompted evaluation of possible effects of this compound on Hsp70 chaperones. There was no evidence for ubiquitinylation of the heat shock cognate protein (Hsc70), a member of the Hsp70 family of chaperones, after cell treatment with hypericin neither for 48 h nor for 72 h in DA3 or SQ2 cells (data not shown). Conversely, Hsc70 increased in content in hypericin-treated DA3 cells at doses that induced Hsp90-ubiquitinylation at the 48- and 72-h time points (Fig. 5A, 3rd left and right panels, respectively). In SQ2 cells the levels of Hsc70 remained unchanged (Fig. 5B, bottom panel). Thus, hypericin-mediated chaperone ubiquitinylation appears to be unique to Hsp90.

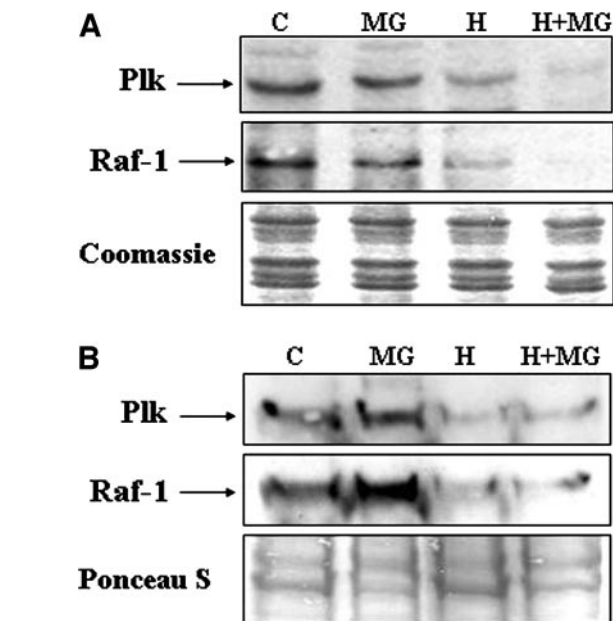


Fig. 3. The role of the proteasome in hypericin-induced turnover of Plk and Raf-1. DA3 cells treated with 10  $\mu\text{M}$  of hypericin for 72 h received MG132 for the last 48 h of the treatment schedule. Levels of Plk and Raf-1 were analyzed by immunoblotting in *A*, NP40 soluble and *B*, in detergent insoluble cell fractions. Coomassie blue and Ponceau S staining are shown to demonstrate equal loading on gels. *C*, denotes untreated cells, *MG* refers to MG132 treated cells, *H* to hypericin treated cells and *H+MG* to the combined treatment with hypericin and MG132.

## DISCUSSION

MCD, which can be generated by the action of exogenous agents, occurs after diminution in functions of several cellular signaling

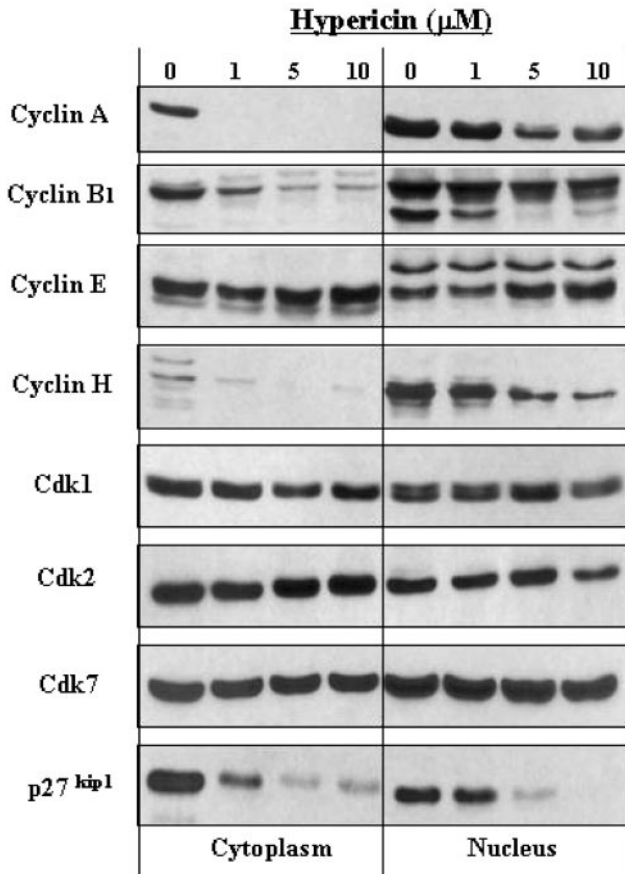


Fig. 4. Changes in cell cycle regulators induced by hypericin. Nuclear and cytoplasmic extracts obtained from DA3 cells exposed to 1–10  $\mu\text{M}$  hypericin for 72 h in the dark were loaded and separated on 10–12% SDS-PAGE. Western blots were prepared using antibodies directed against multiple cyclins, Cdks, and p27<sup>kip1</sup>.

pathways. Their effects neutralize the G<sub>1</sub>-S checkpoint, delay cells at G<sub>2</sub>-M, lead to formation of enlarged cells, and generate multinucleation (5). The different pathways that elicit MCD appear to be unrelated and to involve mutually exclusive molecular players, requir-

ing the existence of a mechanism that can link together these different aberrant functions.

We found that hypericin induces MCD in various tumor cell lines after treatment for 48–72 h in the dark. This model was used to identify mechanisms that can generate the multitargeted deficiencies leading to MCD.

We show that cell exposure to hypericin accelerates turnover and leads to diminution in the content of Cdk4, mutant p53, Raf-1, and Plk (Fig. 2, A and B); others noted reduced cellular levels of ErbB2 in ovary carcinoma cells (11). All are client proteins of the Hsp90 chaperone. Catabolism of Hsp90 client proteins also affected their downstream signaling targets as shown for Raf-1, the turnover of which resulted in diminished activation of Erk type MAP kinases (Fig. 2C). Because Hsp90 client proteins participate in G<sub>1</sub> cyclin activities, G<sub>1</sub>-S cell cycle phase transition checkpoints, and various cellular signaling pathways, reducing their levels can promote cell entry into aberrant cycling, lead to premature mitosis (19, 20), and culminate in MCD.

A prominent role in cell failure to complete M phase-related events in MCD is played by Plk. Plk regulates centrosome maturation (29, 30), bipolar spindle formation (30, 31), microtubule-contraction, cdc2 activation (32), anaphase promoting complex activity (33), and cytokinesis (34, 35). Depletion of Plk or mutations in its substrates have been shown to increase the frequency of multinucleated cells (30, 36). Destabilization of Plk after treatment of tumor cells with hypericin (Fig. 2) appears to generate similar deficiencies in Plk-dependent functions that culminate in MCD.

Another Hsp90 client protein, the destabilization of which can potentially contribute to mitotic catastrophe, is Wee1. This cell cycle checkpoint regulator acts to protract G<sub>2</sub> and prevent immature cell entry into mitosis (37). Loss of Wee1 kinase activity can increase the propensity of cells to enter premature mitosis and consequently to generate the MCD phenomenon.

Analyses of the causes for inactivation of Hsp90 chaperone activity, also exemplified by diminished interaction between Hsp90 and the p50<sup>cdc37</sup> cochaperone (Fig. 5D), revealed that hypericin induces ubiquitinylation of Hsp90 (Fig. 5, A and B). This effect appears to be exclusive to Hsp90 and not to affect Hsp70 chaperones. Conversely, cell content of the cognate Hsc70 increased in hypericin-treated cells

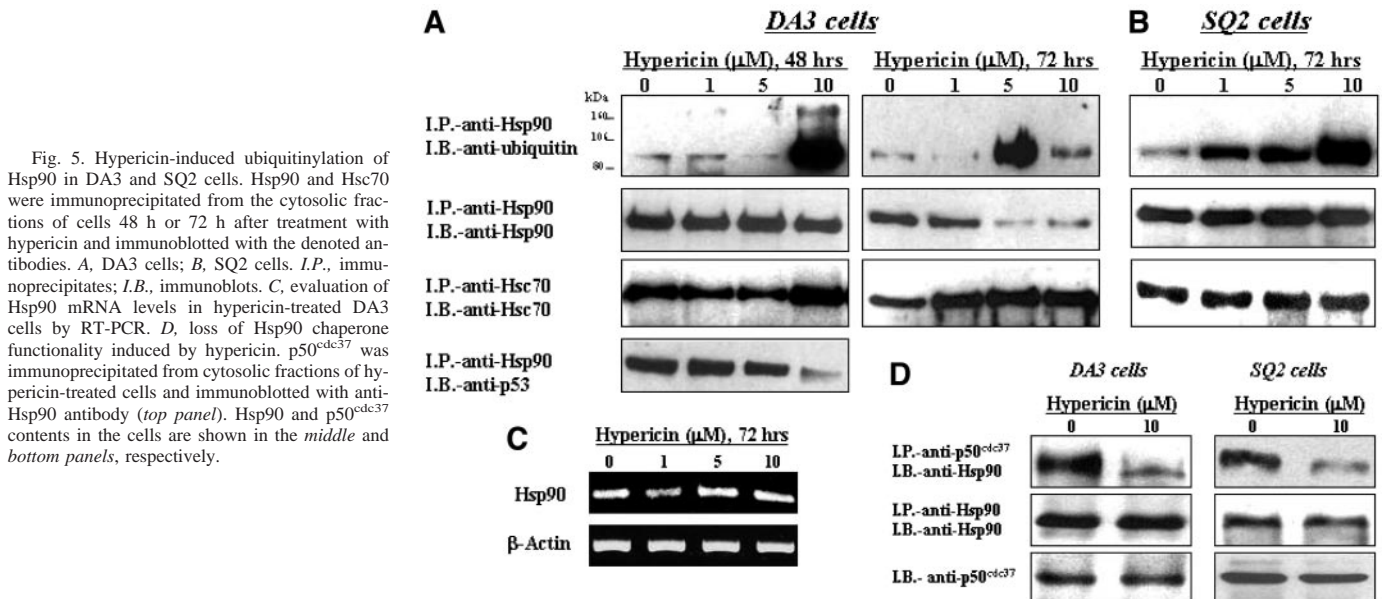


Fig. 5. Hypericin-induced ubiquitinylation of Hsp90 in DA3 and SQ2 cells. Hsp90 and Hsc70 were immunoprecipitated from the cytosolic fractions of cells 48 h or 72 h after treatment with hypericin and immunoblotted with the denoted antibodies. A, DA3 cells; B, SQ2 cells. I.P., immunoprecipitates; I.B., immunoblots. C, evaluation of Hsp90 mRNA levels in hypericin-treated DA3 cells by RT-PCR. D, loss of Hsp90 chaperone functionality induced by hypericin. p50<sup>cdc37</sup> was immunoprecipitated from cytosolic fractions of hypericin-treated cells and immunoblotted with anti-Hsp90 antibody (top panel). Hsp90 and p50<sup>cdc37</sup> contents in the cells are shown in the middle and bottom panels, respectively.

in a manner similar to the effects of geldanamycin, another Hsp90 inhibitor (38).

The hypericin-induced enhanced turnover of Hsp90 client proteins was accompanied by changes in the cellular content of several additional positive cell cycle regulators. Cyclin A, cyclin B1, and cyclin H were found to decline, whereas the content of cyclin E was elevated (Fig. 4). Similar modulations in cell cycle regulators were reported after cell treatment with depsipeptide FR901228 (FK228), a histone deacetylase inhibitor (39). Depsipeptide inactivates Hsp90 by acetylation, leading to depletion of Hsp90 client proteins. These changes are also accompanied by a secondary decrease in cyclin A and elevation of cyclin E (39).

The diminishing cellular content of p27<sup>kip1</sup> observed in this study (Fig. 4) may result from the G<sub>2</sub>-M phase arrest caused by hypericin. p27<sup>kip1</sup> was reported to interact with Hsc70 in a cell cycle-dependent manner with maximal binding at the G<sub>1</sub>-S transition (40). Prolonged cell sequestration in S phase and G<sub>2</sub>-M may have prevented this interaction and accelerated p27<sup>kip1</sup> degradation (41).

Thus, hypericin emerges as a new class of Hsp90 inhibitors that differs from others in the mode by which it affects this chaperone and in the form of cell death that it induces. Unlike geldanamycin and radicicol, which inactivate Hsp90 through interaction with the ADP/ATP binding pocket (18, 38, 42, 43), or depsipeptide (FK228), which induces Hsp90 acetylation (39), hypericin inactivates the chaperone via ubiquitinylation.

An additional dissimilarity between the activities of hypericin and other Hsp90 inhibitors is in the mechanism of protein elimination. In contrast to geldanamycin and radicicol, in which Hsp90 client proteins can be rescued in the presence of MG132 (44), administration of this proteasome inhibitor to hypericin-treated cells is shown to have no effect on accumulation of Hsp90 client proteins in detergent-insoluble fractions (Fig. 3B) as seen with other Hsp90 inhibitors. These differences may result from reduction in intracellular pH known to be elicited by hypericin (15). The reduced pH appears to activate lysosome-mediated protein degradation. Alternatively, proteasome susceptibility to MG132 may diminish under the reduced pH conditions.

The profound differences between the effects of hypericin and those of other Hsp90 inhibitors also extend to the mode of cell death that is induced. Whereas geldanamycin and depsipeptide mainly induce apoptosis (18, 39), hypericin is shown here to cause MCD. The reasons for these disparities are at present unclear. The reduced intracellular pH caused by hypericin might affect caspase activation. It may also be the cause for the reduced catabolism of Plk seen in the pulse/chase experiments during the first 48 h (Fig. 2D), whereas the dramatic shift to accelerated catabolism noted at 72 h may be the outcome of Hsp90 ubiquitinylation, noted to occur after 48–72 h of exposure to hypericin (Fig. 5, A and B).

The anticancer activities of hypericin in the dark may, thus, be viewed in the context of inducing Hsp90 inactivation via ubiquitinylation, leading to destabilization of Hsp90 client proteins culminating in MCD.

## REFERENCES

- Wang, X., Masters, J. R., Wong, Y. C., Lo, A. K., and Tsao, S. W. Mechanism of differential sensitivity to cisplatin in nasopharyngeal carcinoma cells. *Anticancer Res.*, *21*: 403–408, 2001.
- Come, M. G., Skladanowski, A., Larsen, A. K., and Laurent, G. Dual mechanism of daunorubicin-induced cell death in both sensitive and MDR-resistant HL-60 cells. *Br. J. Cancer*, *79*: 1090–1097, 1999.
- Torres, K., and Horwitz, S. B. Mechanisms of Taxol-induced cell death is concentration-dependent. *Cancer Res.*, *58*: 3620–3626, 1998.
- Zhivotovsky, B., Bertrand, J., and Orrenius, S. Tumour radiosensitivity and apoptosis. *Exp. Cell Res.*, *248*: 10–17, 1999.
- Erenpreisa, J., and Cragg, M. S. Mitotic death: a mechanism of survival? *Cancer Cell Internat.*, *1*: 1–7, 2001.
- Gragi, G. Cell cycle regulation of DNA replication. The endoreduplication perspective (minireview). *Exp. Cell Res.*, *244*: 372–378, 1998.
- Joensuu, H., and Dimitrijevic, S. Tyrosine kinase inhibitor imatinib (STI571) as an anticancer agent for solid tumours. *Ann. Med.*, *33*: 451–455, 2001.
- Takahashi, I., Nakanishi, S., Kobayashi, E., Nakano, H., Suzuki, K., and Tamaoki, T. Hypericin and pseudohypericin specifically inhibit protein kinase C: possible relation to their antiretroviral activity. *Biochem. Biophys. Res. Commun.*, *165*: 1207–1212, 1989.
- Agostinis, P., Donella-Deana, A., Cuveele, J., Vandenbogaerde, A., Sarno, S., Merlevede, W., and de Witte, P. A comparative analysis of the photosensitized inhibition of growth-factor regulated protein kinases by hypericin-derivatives. *Biochem. Biophys. Res. Commun.*, *220*: 613–617, 1996.
- Blank, M., Mandel, M., Hazan, S., Keisari, Y., and Lavie, G. Anti-cancer activities of hypericin in the dark. *Photochem. Photobiol.*, *74*: 120–125, 2001.
- Hwang, M. S., Yum, Y. N., Joo, J. H., Kim, S., Lee, K. K., Gee, S. W., Kang, H. I., and Kim, O. H. Inhibition of c-erbB-2 expression and activity in human ovarian carcinoma cells by hypericin. *Anticancer Res.*, *21*: 2649–2655, 2001.
- Lavie, G., Meruelo, D., Aroyo, K., and Mandel, M. Inhibition of the CD8 T cell-mediated cytotoxicity reaction by hypericin. Potential for treatment of T-cell mediated diseases. *Int. Immunol.*, *12*: 479–486, 2000.
- Lavie, G., Valentine, F., Levin, B., Mazur, Y., and Gallo, G. Studies of the mechanisms of action of the antiretroviral agents hypericin and pseudohypericin. *Proc. Natl. Acad. Sci. USA*, *86*: 5963–5967, 1989.
- Moraleda, G., Wu, T. T., Jilbert, A. R., Aldrich, C. E., and Condreay, L. D. Inhibition of duck hepatitis B virus replication by hypericin. *Antiviral Res.*, *20*: 235–247, 1993.
- Sureau, F., Miskovsky, P., Chinsky, L., and Turpin, P. Y. Hypericin-induced cell photosensitization involves an intracellular pH decrease. *J. Am. Chem.*, *118*: 9484–9487, 1996.
- Tcherkasskaya, O., and Uversky, V. N. Denatured collapsed states in protein folding: example of apomyoglobin. *Proteins*, *44*: 244–254, 2001.
- Uzdensky, A. B., Ma, L. W., Iani, V., Hjortland, G. O., Steen, H. B., and Moan, J. Intracellular localisation of hypericin in human glioblastoma and carcinoma cell lines. *Lasers Med. Sci.*, *16*: 276–283, 2001.
- Necker, L. Hsp90 inhibitors as novel cancer chemotherapeutic agents. *Trends Mol. Med.*, *8*: S55–S61, 2002.
- Richter, K., and Buchner, J. Hsp90: Chaperoning signal transduction. *J. Cellul. Physiol.*, *188*: 281–290, 2001.
- Helmbrecht, K., Zeise, E., and Rensing, L. Chaperones in cell cycle regulation and mitogenic signal transduction: a review. *Cell Prolif.*, *33*: 341–365, 2000.
- Simizu, S., and Osada, H. Mutations in the Plk gene lead to instability of Plk protein in human tumour cell lines. *Nature Cell Biol.*, *2*: 852–854, 2000.
- Piper, P. W. The Hsp90 chaperone as a promising drug target. *Curr. Opin. Investig. Drugs*, *2*: 1606–1610, 2001.
- Bartek, J., Iggo, R., Gannon, J., and Lane, D. P. Genetic and immunochemical analysis of mutant p53 in human breast cancer cell lines. *Oncogene*, *5*: 893–899, 1990.
- Gannon, J. V., Greaves, R., Iggo, R., and Lane, D. P. Activating mutations in p53 produce a common conformational effect. A monoclonal antibody specific for the mutant form. *EMBO J.*, *9*: 1595–1602, 1990.
- King, F. W., Wawrzynow, A., Hohfeld, J., and Zyllicz, M. Co-chaperones Bag-1, Hop and Hsp40 regulate Hsc70 and Hsp90 interactions with wild-type or mutant p53. *EMBO J.*, *20*: 6297–6305, 2001.
- Pelech, S. L., and Charest, D. L. MAP kinase dependent pathways in the cell cycle control. *Prog. Cell Cycle Res.*, *1*: 33–52, 1995.
- Martinez, A. M., Afshar, M., Martin, F., Cavadore, J. C., Labbe, J. C., and Doree, M. Dual phosphorylation of the T-loop in cdk7: its role in controlling cyclin H binding and CAK activity. *EMBO J.*, *16*: 343–354, 1997.
- Kato, J. Y., Matsuoka, M., Strom, D. K., and Sherr, C. J. Regulation of cyclin D-dependent kinase 4 (cdk4) by cdk4-activating kinase. *Mol. Cell Biol.*, *14*: 2713–2721, 1994.
- Gonzalez, C., Sunkel, C. E., and Glover, D. M. Interactions between *mgr*, *asp*, and *polo*: *asp* function modulated by *polo* and needed to maintain the poles of monopolar and bipolar spindles. *Chromosoma*, *107*: 452–460, 1998.
- Lane, H. A., and Nigg, E. A. Antibody microinjection reveals an essential role for human polo-like kinase 1 (Plk1) in the functional maturation of mitotic centrosomes. *J. Cell Biol.*, *135*: 1701–1713, 1996.
- Llamazares, S., Moreira, A., Tavares, A., Girdham, C., Spruce, B. A., Gonzalez, C., Karess, R. E., Glover, D. M., and Sunkel, C. E. Polo encodes a protein kinase homolog required for mitosis in *Drosophila*. *Genes Dev.*, *5*: 2153–2165, 1991.
- Ouyang, B., Li, W., Pan, H., Meadows, J., Hoffmann, I., and Dai, W. The physical association and phosphorylation of Cdc25C protein phosphatase by Prk. *Oncogene*, *18*: 6029–6036, 1999.
- Descombes, P., and Nigg, E. A. The polo-like kinase Plx1 is required for M phase exit and destruction of mitotic regulators in *Xenopus* egg extracts. *EMBO J.*, *17*: 1328–1335, 1998.
- Carmera, M., Riparbelli, M. G., Minestrini, G., Tavares, A. M., Adams, R., Callaini, G., and Glover, D. M. *Drosophila* polo kinase is required for cytokinesis. *J. Cell Biol.*, *143*: 659–671, 1998.
- Song, S., Grefell, T. Z., Garfield, S., Erikson, R. L., and Lee, K. S. Essential function of the polo box of Cdc5 in subcellular localization and induction of cytokinetic structures. *Mol. Cell Biol.*, *20*: 286–298, 2000.
- Yarm, F. Plk phosphorylation regulates the microtubule-stabilizing protein TCTP. *Mol. Cell Biol.*, *22*: 6209–6221, 2002.
- Wang, Y., Li, J., Booher, R. N., Kraker, A., Lawrence, T., Leopold, W. R., and Sun, Y. Radiosensitization of p53 mutant cells by PD0166285, a novel G(2) checkpoint abrogator. *Cancer Res.*, *61*: 8211–8217, 2001.

38. Huang, H. C., Liu, Y. C., Liu, S. H., Tzang, B. S., and Lee, W. C. Geldanamycin inhibits trichostatin A-induced cell death and histone H4 hyperacetylation in COS-7 cells. *Life Sci.*, *70*: 1763–1775, 2002.
39. Yu, X., Guo, S. Z., Marcu, M. G., Neckers, L., Nguyen, D. M., Chen, G. A., and Schrump, D. S. Modulation of p53, ErbB1, ErbB2 and Raf-1 expression in lung cancer cells by depsipeptide FR901228. *J. Nat. Cancer Inst.*, *94*: 504–513, 2002.
40. Nakamura, S., Tatuno, I., Noguchi, Y., Kitagawa, M., Kohn, L. D., Saito, Y., and Hirai, A. 73-kDa heat shock cognate protein interacts directly with p27kip1, a cyclin-dependent kinase inhibitor, during G1/S transition. *Biochem. Biophys. Res. Commun.*, *257*: 340–343, 1999.
41. Pagano, M., Tam, S. W., Theodoras, A. M., Beerromero, P., Del Sal, G., Chau, V., Yew, P. R., Draetta, G. F., and Rolfe, M. Role of the ubiquitin-proteasome pathway in regulating abundance of the cyclin-dependent kinase inhibitor p27. *Science (Wash. DC)*, *269*: 682–685, 1995.
42. Hostein, I., Robertson, D., DiStefano, F., Workman, P., and Clarke, P. A. Inhibition of signal transduction by the Hsp90 inhibitor 17-allylamino-17-demethoxygeldanamycin results in cytostasis and apoptosis. *Cancer Res.*, *61*: 4003–4009, 2001.
43. Schneider, C., Sepp-Lorenzino, L., Nimmegern, E., Ouerfelli, O., Danishefsky, S., Rosen, N., and Hartl, F. U. Pharmacologic shifting of a balance between protein refolding and degradation mediated by Hsp90. *Proc. Natl. Acad. Sci. USA*, *93*: 14536–14541, 1996.
44. Meriin, A. B., Gabai, V. L., Yaglom, J., Shifrin, V. I., and Sherman, M. Y. Proteasome inhibitors activate stress kinases and induce Hsp72. Diverse effects on apoptosis. *J. Biol. Chem.*, *273*: 6373–6379, 1998.